

---

# Large Eddy Simulation of turbulent flows around a rotor blade segment using a Spectral Element Method

A. Shishkin<sup>1</sup> and C. Wagner<sup>2</sup>

<sup>1</sup> Institute for Aerodynamics and Flow Technology, DLR – German Aerospace Center, Göttingen, Germany [Andrei.Shishkin@dlr.de](mailto:Andrei.Shishkin@dlr.de)

<sup>2</sup> Institute for Aerodynamics and Flow Technology, DLR – German Aerospace Center, Göttingen, Germany [Claus.Wagner@dlr.de](mailto:Claus.Wagner@dlr.de)

## Summary

Large Eddy Simulations (LES) of turbulent flows around a segment of the FX-79-W151 airfoil have been performed for different Reynolds numbers between  $Re = 5 \cdot 10^3$  and  $Re = 10^5$  and the angle of attack  $12^\circ$  using a Spectral Element Method (SEM). The results of the LES for  $Re = 5 \cdot 10^3$  and  $Re = 5 \cdot 10^4$  are compared. The turbulence statistics obtained in the LES reveal laminar and turbulent flow separation regions for the lower and higher Reynolds numbers, respectively.

## 1 Numerical method and computational parameters

Numerical methods based on Reynolds-Averaged Navier-Stokes (RANS) equations are successfully applied for a wide range of industrial applications. Nevertheless, many unsteady flow problems dealing with complex three-dimensional domains can not be accurately simulated in the framework of statistical turbulence modeling due to unsteady nature of the problem. In this respect, the Large Eddy Simulation (LES) has proven to be a promising technique.

Here we present the results obtained in LES of the turbulent flow around a segment of the FX-79-W151 profile with an angle of attack  $\alpha = 12^\circ$ . The early results of the simulation for  $Re = 5 \cdot 10^3$  and some related questions were discussed in [4]. We use the spectral/hp element method based on the high order 2D polynomial representation of the solution combined with the Fourier extension in homogenous spanwise direction. This method was developed by Karniadakis, Sherwin (1999) [1] and co-workers and implemented in the ***N** $\epsilon$ ***\kappa*T** $\alpha$ **r*** code.

The LES is governed by the dimensionless incompressible filtered Navier-Stokes equations together with the Smagorinsky subgrid scale model adapted to high order SEM by Karamanos [2].

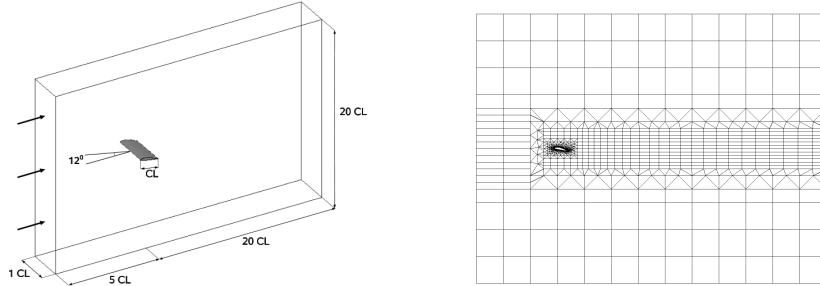


**Fig. 1.** Schematic view of the computational domain (left) and unstructured 2D mesh (right) consisting of 2116 elements.

The computational domain is schematically shown in Fig.1 (left). The size of the computational domain is  $25cl \times 20cl \times 1cl$  ( $cl$  denotes the chord length) in streamwise, vertical and spanwise directions, respectively. We use time-independent laminar inflow boundary conditions, Neumann boundary conditions at the outflow boundary and periodic conditions in spanwise direction. We implemented the sponge zone in order to damp the turbulent vortical structures at the outflow boundary.

The LES are carried out for the Reynolds numbers based on the chord length and the freestream velocity  $Re = 5 \cdot 10^3$ ,  $Re = 5 \cdot 10^4$  and  $Re = 10^5$  on the hybrid structured/unstructured mesh consisting of 2116 2D-elements (Fig.1, right) with 64 Fourier planes in spanwise direction. The polynomial order  $P = 9$  yields about  $5.5 \cdot 10^6$  degrees of freedom.

The simulations are performed on 64-bit Linux Cluster with 1.7GHz AMD Opteron processors. The memory usage is 20G and one time step takes approximately 5.5 CPU seconds on 32 processors. The computational expenses of the SEM in this "2D+Fourier" case are much lower than those in "full 3D" SEM considered in [3].

## 2 Results of Large Eddy Simulations

The flow fields predicted in the LES are averaged in time and over the spanwise length to get the turbulence statistics. Some of the results are depicted in Fig.2-3.

The mean streamwise velocity components (Fig.2) reveal the flow acceleration over the leading edge and the backflow regions (outlined with white curves) for both Reynolds numbers. One can observe that the backflow region is closer to the leading edge for the higher Reynolds number.

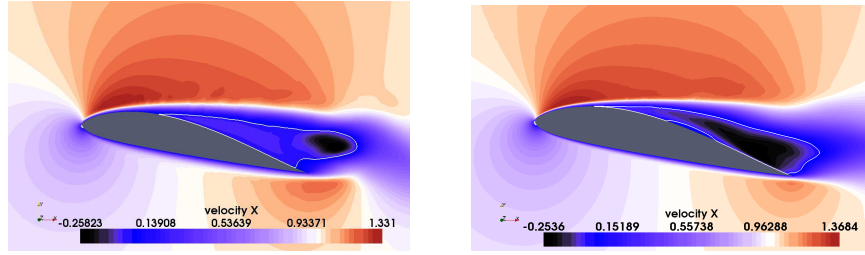


**Fig. 2.** The mean streamwise velocity components as obtained in the LES for  $Re = 5 \cdot 10^3$  (left) and for  $Re = 5 \cdot 10^4$  (right). The regions of negative mean velocity (backflow) are outlined.

The turbulent kinetic energy (TKE) (Fig.3) reveals an essential difference between the two studied cases. The zone of higher TKE is located downstream the trailing edge for  $Re = 5 \cdot 10^3$ . In the case of the higher Reynolds number this zone is located in the suction side area close to the trailing edge.

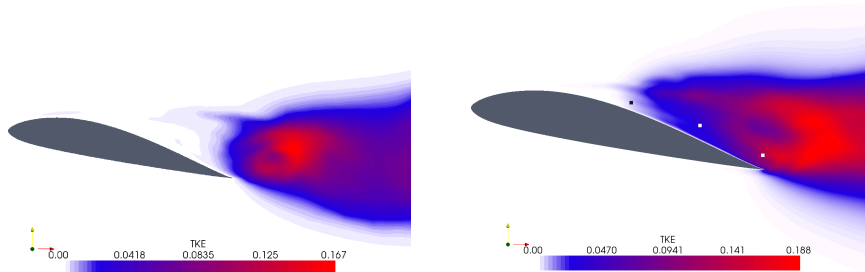


**Fig. 3.** Distributions of the turbulent kinetic energy obtained in the LES for  $Re = 5 \cdot 10^3$  (left) and  $Re = 5 \cdot 10^4$  (right).

Considering both, the distributions TKE and the mean streamwise velocity components, one concludes that flow separation is observed for both Reynolds numbers, but a turbulent separation is predicted for the higher Reynolds number while the separation is laminar for the lower one. The further analysis of the spatial energy spectra at three locations over the suction side of the rotor blade marked in Fig.3 (right) confirms the conclusions. The locations have been chosen as follows: position one is in a region where high TKE values are observed for both Reynolds numbers (right point in Fig. 3); at position two (middle point in Fig. 3) large TKE values are obtained only for the higher Reynolds number; finally, position three (left point in Fig. 3) is located in a low TKE region for both cases. Energy spectras taken in the higher TKE region (Fig. 4, middle and right top and right bottom) reflect a decay which partly agrees with the Kolmogorov  $-5/3$  law of turbulence, while the spectras

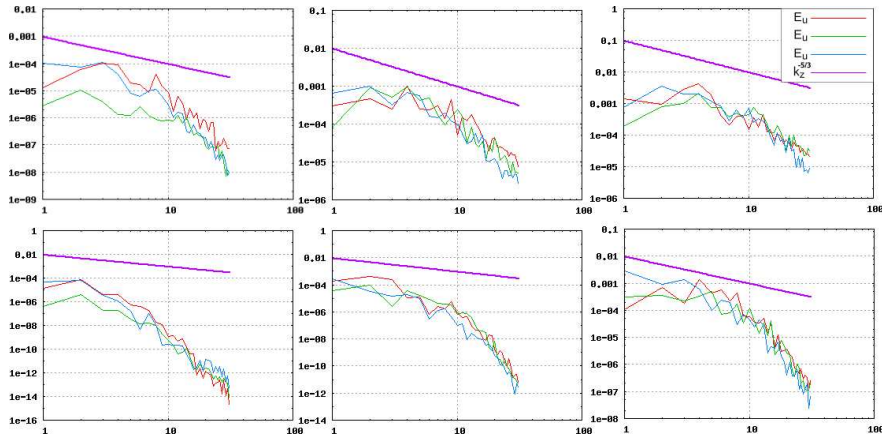


**Fig. 4.** Energy spectra components for  $Re = 5 \cdot 10^4$  (top) and  $Re = 5 \cdot 10^3$  (bottom) at the three positions above the trailing edge in Fig. 3. The ordering from left to right corresponds to that on Fig. 3.

taken at the other locations are characterized by low energy values and faster decay for all components.

### 3 Outlook and future work

The above presented results are obtained in LES of turbulent separated flows around the rotor blade segment for Reynolds numbers  $Re = 5 \cdot 10^3$  and  $Re = 5 \cdot 10^4$  using SEM. The study of the streamwise velocity components, the distributions of the TKE and the energy spectras at some positions over the suction side reveals a turbulent separation for the higher Reynolds number, while the laminar separation region is observed for the lower Reynolds number.

The LES for  $Re = 10^5$  is currently running. The results for  $Re = 5 \cdot 10^4$  and  $Re = 10^5$  will be compared with experiments in the near future.

### References

1. Karniadakis, G.E. , Sherwin, S. (1999). Spectral/HP Element Methods for CFD. Oxford University Press, Oxford.
2. Karamanos, G.-S.(1999) Large Eddy Simulation Using Unstructured Spectral/hp Elements. PhD Thesis, Imperial College.
3. Shishkin, A., Wagner. C. (2006). Direct Numerical Simulation of a turbulent flow using a spectral/hp element method. *Notes on Numer. Fluid Mech.*, v.92, 405-412, Springer, Germany.
4. Shishkin, A., Wagner. C. (2006). Large eddy simulation of the flow around a wind turbine blade. In Wesseling, P., Onate, E., Periaux, J., eds., *European Conference on Computational Fluid Dynamics*.